A STUDY ON RADIATIVE AND CONVECTIVE HEAT EXCHANGE IN A ROOM WITH FLOOR HEATING

Haruo Hanibuchi
SEKISUI HOUSE LTD.
Kizu, Kyoto 619-0224, JAPAN.
and
Shuichi Hokoi
Kyoto University
Sakyo, Kyoto 606-8501, JAPAN.

ABSTRACT

Several features of heat transfer on enclosing surfaces is discussed including temperature distributions in a room heated by a floor heater. Experiments and numerical analysis on radiative and convective heat transfer were carried out against several partial floor heating. Partial floor heating produces different types of temperature distribution between the heated and non-heated places, which is an remarkable characteristics found out in this study. In the heated places, the temperature distribution is almost the same as that of typical floor heating. However, in the non-heated places, air temperature differs by 2 °C (3.6 °F difference) between a point near the floor surface and a point well above that. Heating efficiency of partial heating slightly depends on the set place as well as its area. Moreover, convective heat exchange constitutes approximately half of the total heat exchange.

INTRODUCTION

When floor heating is applied to an actual room, there needs to be some consideration to heating conditions. Because some part of the occupant's body contacts the floor surface, temperature at the floor surface must be kept relatively low compared with other heating panels. Therefore, a wide heated area is required in order to supply enough heat for the room. Although heating the entire floor surface is desirable, this kind of setup is used seldom; usually only a part of the floor surface is heated. With respect to uniform thermal conditions in the room, such partial heating is not desirable, and it is important to understand how the "partial" floor heating affects the thermal conditions in the room.

There are many studies focusing on performance of floor heating panels. Several basic equations to calculate heat transfers by convection, radiation and those combination are described in ASHRAE Handbook (ASHRAE 1996). In such a radiant heated space, radiative heat exchange is a dominant factor in determining the thermal state in a room with a heated floor. However, the convective heat exchange is not only significantly influenced by the heating condition but it also affects room air temperature directly. Basic performance of a floor heating panel was also discussed in our previous study (Hanibuchi and Hokoi 1998).

In present study, the characteristics of these heat transfers are discussed with respect to air temperature distributions obtained by three experiments in a full-scaled room including two partial floor heating. Numerical analysis on radiative and convective heat transfer are also carried out for detailed discussion.

EXPERIMENTAL PROCEDURE

Apparatus

Experiments were carried out in the model room, schematically shown in Figure 1. It is built inside a large climate chamber kept at a constant temperature of 2°C (35.6 °F). The floor heating system is composed of an electric heater, a pump and piping for hot water circulation, header, and thermostat for controlling hot water temperature. The pipe is embedded uniformly in the floor as shown in Figure 2 (a). Floor construction is shown in Figure 3. Hot water heated by the electric heater is circulated through the piping which is divided into four zones A, B, C, and D by the header shown in Figure 2 (b). The amount of hot water supply to each zone can be controlled independently by the header, although water temperature can not. The water temperature depends on the value set by the electric water heater.

The room air and inside wall surface temperatures, including the air temperature near wall in 55 points at heights of 50 mm (0.16 ft.) and of 600 mm (1.97 ft.) above the floor, were measured at 330 points by a type T (copper-constantan) thermocouples. Because there are many measuring points, it is hard to calibrate all the sensors with sufficient care. Therefore it was simply confirmed that all the measured values were within the range of 1.8 °C (35.24 °F) to 2.8 °C (37.04 °F) when the room air temperature was approximately 2 °C (35.6 °F). Air velocity in the room at 15 points, temperatures of the supplied and returned hot water, as well as the amount of circulated water, were measured. The thermocouples on the wall surface are covered with an air-permeable seal, having almost the same color as the wall surface. Since sensors on the wall surface receive radiative as well as convective heat

flux, the measured surface temperatures is regarded as almost actual. Air temperature was measured by thermocouples with an aluminum cover in order to avoid radiation.

Experimental Conditions

The insulation qualities of the experimental room are shown in Figure 1 as U-values, which were calculated from the respective structural materials. It should be noted that the thermal resistance of the flooring, pipe and joist is not considered in the U-value of the floor. Because discussion in this paper will be limited to the results at a steady state, heat capacity is not necessary. The outside temperature is set at a constant value of 2 °C (35.6 °F). Solar radiation, occupants, obstacle and heat sources except for the floor heating is not considered. The steady state heat load calculated using U-values is 1367 W (4664 Btu/h), when the difference between the outside and inside temperatures is set at 18 °C (64.4 °F). Air change rate by natural ventilation is approximately 0.5, which was obtained by measurement when the floor was heated.

The measurements were carried out under three different heating conditions. That is, the case of the entire floor surface being heated (zones A, B, C and D), part of the floor being heated (center zones represented by B and C) and another part of the floor being heated (zones represented by A and B). In each case, the floor surface temperature is controlled within the range of 20°C (68.0°F) to 30°C (86.0°F). Thus, enough heat can be supplied in order to keep the average room air temperature to 20°C (68.0°F). These conditions are listed in Table 2.

NUMERICAL PROCEDURE

Numerical analysis on convective and radiative heat transfer was conducted with respect to the two measured temperature fields and heat loads of Case 1 and Case 3. Convective and radiative heat transfer analyses were carried out independently by using the measured surface temperatures. The computational results obtained by the following procedure will be discussed later, along with the experimental results.

Analysis of Convective Heat Transfer

Three-dimensional convective heat transfer was analyzed by using the k-ε turbulence model and computational boundary conditions shown in Appendix A (Hanibuchi and Hokoi 1996). Boundary conditions, which was referred to in previous studies (Hanibuchi and Hokoi 1996, Launder 1988, Murakami et al. 1995, Yürges 1924), were chosen after several numerical tests. Measured surface temperatures were used as the boundary value in computations, and the room air temperature and velocity can be computed. The inside space is divided into 25,536 cells (28*38*24) in computations.

Analysis of Radiative Heat Transfer

Long-wave radiative heat transfer between room surfaces was analyzed by using the basic equations of inter-reflection shown in Appendix B. Every surface is assumed completely diffusive and the emissivity of the windows and the other walls is set at 0.95 and 0.90, respectively. Inside surfaces are divided into 3 cells in the x-direction, 7 cells in the y-direction and 4 cells in the z-direction.

RESULTS AND DISCUSSIONS

Following are the experimental and numerical results, and discussions on temperature and heat load, as well as details on heat exchange. Operative temperature is also mentioned briefly. Velocity results are not discussed in this paper, however, it must be better to mention that the maximum velocity is appropriate 0.1m/s (0.33 ft/s) which was measured near the largest window.

Comparison among Experimental Results

Table 2 shows three experimental results of heat supply/loss and several defined temperatures. The outdoor temperatures are set at the same value of 2.6 °C (36.7 °F) in all cases. While average room air temperatures in Case 1 and Case 2 are approximately the same, that in Case 3 is 2 °C degrees (3.6 °F difference) lower than other two cases. Because the floor surface temperature is controlled so as not to exceed 30 °C (86.0 °F), the heat supply from the floor is not sufficient enough to keep the floor temperature at 20 °C (68.0 °F) in Case 3. The value of MRT, which is replaced approximately by the average enclosing surface temperature, are lower than the average room air temperature by 1 °C degree (1.8 °F difference) in all cases. The operative temperatures are almost middle values between MRT and room air temperature. These results are typical of conventional radiant heating. However, the temperature in Case 3 is too low. The heat supply is approximately proportional to the temperature difference between outdoor and indoor in Case 1 and Case 2. The energy required for a 1 °C degree (1.8 °F difference) increase in room air temperature is 63.6 W/K (120.5 Btu/h°F) in Case 1 and 64.1 W/K (121.4 Btu/h°F) in Case 2. However, more energy is needed in Case 3 (68.6 W/K (129.9 Btu/h°F)) than in other cases, as shown in Table 2. The results clearly shows the heating efficiency of partial heating slightly depends on the set place as well as its area.

Vertical and Horizontal Temperature Distributions

The experimental vertical temperature profiles in the three cases are compared in Figure 4.

The measured room air temperature in Case 1 is almost uniform in the vertical direction, which is typical of a radiative heating system such as floor heating. However, the air temperature at the height of 2,400 mm (94.49 ft.) , near the ceiling, is slightly higher than that at other heights between 50 mm (1.97 ft.) and 1,800 mm (70.87 ft.). This indicates the room air is slightly stratified. The measured result at point P1 near the window shows a low temperature due to cold drafts from the window. This influence is further emphasized

in Case 2. This indicates that the cold draft can not be eliminated because of the lack of heating near the windows. The temperature profiles in Case 3 are significantly different from other cases. Air temperature in the heated area (represented by P1) is almost uniform in the vertical direction, which is common to Case 1 and Case 2. But, the temperature in non-heated areas (represented by P3) is not uniform at all, and the temperature near the floor is lower than that of the upper part at 1,200 mm (47.24 ft.) or 1,800mm (70.87 ft.) in height by 2 °C degrees (3.6 °F difference). The floor surface temperature is much lower. The same trend can be seen in the experimental result where an air-conditioner is used (Hanibuchi and Hokoi 1996). Also, around the center of the room (represented by P2), the air temperature near the floor surface is slightly lower than that in the upper part. It must be due to the cold draft flowing from the non-heated area into the heated area. This is a remarkable characteristics of partial floor heating found out in this study.

Calculated vertical temperature profiles in Case 1 and Case 3 are shown in Figure 5. The average value across the entire plane is used to plot the profile for each height. The calculated temperatures are slightly lower than the experimental results. The same tendency can be seen when an air-conditioner is used (Hanibuchi and Hokoi 1996). The difference between the experimental and numerical results is mainly due to the approximations introduced into the calculation procedures, although it may be partly due to experimental error. For example, sensitivity analysis for room air temperature when an air-conditioner is used indicates that a temperature deviation of 1 °C degree (1.8 °F difference) is possible depending on the boundary condition employed. It is concluded from these analyses that the boundary condition used here is one which may have as similar potential for a forced convection air flow as others generally used. Obtained results agree well with the experiment in some part. However, a temperature deviation of 1 °C degree (1.8 °F difference) may not be ignored and it should be investigated further.

Figure 6 illustrates the experimental air temperature distributions across horizontal planes 50 mm (1.97 ft.) and 600 mm (23.62 ft.) above the floor. The header assembled in the room shown in Figure 2 is covered with thick thermal insulation (like box) to avoid heat leakage. However, some of the air temperature sensors adjacent to the header is also covered by the insulation. These sensors indicate slightly high values, affected by the header, which should be eliminated or revised. Therefore, the contour is drawn after these singular data sets is replaced by the average values at neighboring points.

Except for the region near the windows, the air temperature distribution in Case 1 is almost uniform. However, low air temperature regions due to cold drafts can be seen near the windows corresponding to the vertical temperature profiles (See Figure 4). In Case 2 and Case 3, the distributions are largely affected by the relative position of the heated area. In Case 2, the temperature is about 20 °C (68.0 °F) around the heated center area of the room, while it is slightly low in the non-heated window side area. Furthermore, the distribution in Case 3 shows quite different characteristics between the left and right side of the room; these areas correspond to the heated and unheated areas. However, it should be mentioned that the temperature distribution within each plane is almost uniform in both parts. These distributions are highly affected by radiation. Furthermore, these results seem to indicate that the influence of convection cannot be ignored. These results can be regarded as the same trend seen in the vertical temperature profile.

The numerical results in Case 1 and Case 3 are shown in Figure 7 in a similar fashion to Figure 6. The numerical results compare to the measured distribution well, however the calculated temperatures are approximately by 1 °C degree (1.8 °F difference) lower than the experimental results for most of the room. As mentioned before, the difference between the results may be due to the film coefficient used in boundary condition being to large. Since the value of the film coefficient depends on the calculated velocity near the enclosure, temperatures are also influenced by the velocity. Further study must be done before concluding whether the difference between the numerical and experimental results is caused mainly by the film coefficient formula or the velocity result.

Heat Exchange on Inside Surface

Table 3 shows the amount of heat exchange on inside surfaces, obtained by experiment and calculation. The experimental results are obtained based on the temperature difference between the inside wall surface and outdoor air, and the conductance between them.

$$Q = \sum q_i S_i + c\gamma Vn(\theta_r - \theta_o) \quad (1)$$

$$q_i = D_m(\theta_w - \theta_o) \quad (2)$$

$$R_m = 1/D_m = r_w + 1/\alpha_o \quad (3)$$

Measured values of heat loss are evaluated assuming that the heat exchange takes place on every inside surface except for the heated floor surface. Total heat loss can be determined by summing them up in addition to the heat lost by natural air change. The positive value indicates heat flow from room air to the inside surface for convective heat flux, and the net absorbed heat on the inside surface for radiative heat flux. Therefore, the positive values mean heat loss from the room. Since it is difficult to estimate the radiative and convective heat fluxes separately from the measured data, only the sum of radiative and convective heat fluxes is listed in Table 3 as the experiment-drawn values.

Heat loss by natural ventilation should be considered in convective heat transfer analysis, however, it is not in this study. The sum of the radiative

heat fluxes for all surfaces combined should be zero. Although the numerical results are not exactly zero, the differences are small enough to be neglected as computational error.

The common trend in both cases (Case 1 and Case 3) is that the heat loss by radiative heat exchange through each surface comes within the range of 50 % to 60 %, except for the ceiling. Radiative heat exchange is more on the ceiling surface and it is over 60 %. This percentage exceeds that in total heat loss, which is a typical feature of radiative heat exchange related to floor panel heating. Any significant difference in heat exchange characteristics can not be seen in either case. However, the ratio of convective or radiative heat exchange of Wall-1 to the total heat loss is slightly different between two cases. This difference causes the different heating efficiency between them shown in Table 2. The heating efficiency of partial heating is slightly affected by the set place as well as its area.

In both cases, the calculated total heat loss is in good agreement with the measured values. However, the calculated results slightly overestimate the total heat loss just by the amount of ventilation as mentioned above. The sum of the convective and the radiative heat fluxes on almost all surfaces obtained by numerical calculation is also larger than the experimental result. This can be attributed to the too large film coefficient used in the calculations. This may be the main reason why the calculated average room temperatures are slightly lower than those in experiments.

CONCLUSIONS

This paper presented several features of heat transfer on inside surfaces and temperature distribution in a room with partially heated floor. The following results were obtained.

(1) The floor heating produces an almost uniform air temperature distribution except near windows where cold drafts lower the air temperature.

(2) Partial floor heating produces different types of temperature distribution between the heated and non-heated places. In the heated places, the temperature distribution is almost the same as that of typical floor heating. However, in the non-heated places, air temperature differs by 2 °C degrees (3.6 °F difference) between a point near the floor surface and a point well above that. This is an remarkable characteristics clarified in this study.

(3) While radiative heat exchange plays an important role especially at the ceiling surface, convective heat exchange based on numerical analysis constitutes approximately half of the total heat exchange.

(4) The heating efficiency of partial heating is slightly depends on the set place as well as its area.

REFERENCES

American Society of Heating, Refrigerating, and Air-Conditioning Engineer, Inc. 1996, "ASHRAE HANDBOOK HVAC Systems and Equipments", Atlanta, ASHRAE, CHAPTER 6, pp.6.1-6.20.

Hanibuchi, H. and Hokoi, S. 1996, "Analysis of velocity and temperature fields in a room heated by a room air-conditioner." Proceedings of 5th International Conference on Air Distribution in Rooms, ROOMVENT '96, Vol.1, pp.445-452.

Hanibuchi, H. and Hokoi,S. 1998, "Basic Study on Radiative and Convective Heat Exchange in a Room with Floor Heating." ASHRAE Transactions, Vol.104, part1B, pp.1098-1105.

Launder,B.E. 1988, "On the calculation of convective heat transfer in complex turbulent flows." J. Heat Transfer, Vol.110, pp.1112-1128.

Murakami,S., Kato, S., Kondo, Y., Takahashi, Y. and Dongho,D. 1995, "Numerical study on thermal environment in air-conditioned room by means of coupled simulation of convective and radiative heat transport (Part 1) (in Japanese)." Transactions of the Society of Heating, Air-Conditioning and Sanitary Engineers of Japan, No.57, pp.105-116.

Yürges,W. 1924, "Der Wärmeübergang an einer ebenen Wand (in Germany)." Beihefte zum Gesundheits-Ingenieur, Beiheft 19, pp.1-51.

APPENDIX

[A] Equations for the Convective Heat Transfer

The balance equation for continuity, momentum, and heat are represented by Eq. (A1), (A2), and (A3).

$$\frac{\partial U_i}{\partial x_i} = 0 \tag{A1}$$

$$\frac{\partial U_i}{\partial t} = -\frac{\partial U_i U_j}{\partial x_j} - \frac{\partial \pi}{\partial x_i} + \frac{\partial}{\partial x_j}\left\{(\nu_t + \nu)\left(\frac{\partial U_i}{\partial x_j} + \frac{\partial U_j}{\partial x_i}\right)\right\} + g\beta\theta\delta_{ij} \tag{A2}$$

$$\frac{\partial \theta}{\partial t} = -\frac{\partial \theta U_j}{\partial x_j} + \frac{\partial}{\partial x_j}\left\{\left(\frac{\nu_t}{\sigma_\theta} + a\right)\frac{\partial \theta}{\partial x_j}\right\} \tag{A3}$$

Adding the balance equation for the turbulent kinetic energy and the turbulent energy dissipation represented by Eq. (A4) and (A5) including additional relational formula given by (A6) and (A7) , a set of mathematical model for turbulence are composed.

$$\frac{\partial k}{\partial t} = -\frac{\partial k U_j}{\partial x_j} + \nu_t\left(\frac{\partial U_i}{\partial x_j} + \frac{\partial U_j}{\partial x_i}\right)\frac{\partial U_i}{\partial x_j} + \frac{\partial}{\partial x_j}\left\{\left(\frac{\nu_t}{\sigma_k} + \nu\right)\frac{\partial k}{\partial x_j}\right\} - \varepsilon \tag{A4}$$

$$\frac{\partial \varepsilon}{\partial t} = -\frac{\partial \varepsilon U_j}{\partial x_j} + c_{\varepsilon 1}\frac{\varepsilon}{k}\nu_t\left(\frac{\partial U_i}{\partial x_j} + \frac{\partial U_j}{\partial x_i}\right)\frac{\partial U_i}{\partial x_j} + \frac{\partial}{\partial x_j}\left\{\left(\frac{\nu_t}{\sigma_\varepsilon} + \nu\right)\frac{\partial \varepsilon}{\partial x_j}\right\} - c_{\varepsilon 2}\frac{\varepsilon^2}{k} \tag{A5}$$

$$\nu_t = c_D\frac{k^2}{\varepsilon} \tag{A6}$$

$$\pi = \frac{P}{\rho} + \frac{2}{3}k \tag{A7}$$

Wall boundary conditions used for U_i, k, ε and θ in computation are given by following relations.

$$\left.\frac{\partial U}{\partial y}\right|_{wall} = \frac{1}{7}\frac{U_p}{y_p}, \qquad \left.\frac{\partial k}{\partial y}\right|_{wall} = 0, \qquad \varepsilon_p = \frac{C_D^{\frac{3}{4}} k_p^{\frac{3}{2}}}{\kappa y_p} \tag{A8}$$

$$q_w = \alpha\left(\theta_p - \theta_w\right) \tag{A9}$$

$$\alpha = 5.3 + 3.6\sqrt{U_p} \tag{A10}$$

$$\left.\frac{\partial \theta}{\partial y}\right|_{wall} = \frac{1}{7}\frac{\theta_p - \theta_w}{y_p} \tag{A11}$$

[B] Basic Equations for the Radiative Heat Transfer

If every surface is assumed completely diffusive, the radiation inter-reflection can be expressed by Eq. (B1), net radiative heat flux absorbed by wall is given by Eq.(B2) and sum of the net radiative heat flux must satisfy by Eq.(B3).

$$G(s) = \int_s \varepsilon(s')E_b(s')F(ss')ds' + \int_s [1-\varepsilon(s')]G(s')F(ss')ds' \tag{B1}$$

$$q(s) = \varepsilon(s)\left[G(s) - E_b(s)\right] \tag{B2}$$

$$\int_s q(s)ds = 0 \tag{B3}$$

NOMENCLATURE

a = molecular diffusion coefficient of θ [m²/s] ([ft²/s])
D_m = thermal conductance between inside surface and outdoor temperature [W/m²K] ([Btu/ft²h°F])
$E_b(s)$ = emissive power of a blackbody [W/m²] ([Btu/ft²h])
$F(ss')ds$ = configuration factor (shape factor) [-]
$G(s)$ = irradiation [W/m²] ([Btu/ft²h])
g = gravity [m/s²] ([ft/s²])
k = turbulent kinetic energy [m²/s²] ([ft²/s²])
n = air change rate by natural ventilation [-]
P = pressure [kg/ms²] ([lb/fth²])
$q(s)$ = net radiative heat flux absorbed by wall [W/m²] ([Btu/ft²h])
Q = total heat loss [W] ([Btu/h])
q_i = heat flux at i th cell [W/m²] ([Btu/ft²h])
q_w = heat flux [W/m²] ([Btu/ft²h])
R_m = thermal resistance between i th wall surface and outdoor air layers [m²K/W] ([ft²h°F/Btu])
r_w = thermal resistance of wall [m²K/W] ([ft²h°F/Btu])
S = inside surface area of walls [m²] ([ft²])
S_i = surface area of i th cell [m²] ([ft²])
s, s' = positions at the inside surface of wall
t = time [s]
U_i = velocity in i th direction [m/s] ([ft/s])
V = room volume [m³] ([ft³])
x_i = position in i th direction
y_p = distance from the wall to a node adjacent to wall [m] ([ft])
α = inside film coefficient [W/m²K] ([Btu/ft²h°F])
α_o = outer film coefficient [W/m²K] ([Btu/ft²h°F])
β = coefficient of cubical expansion [1/K]
γ = specific heat of air [W/kgK] ([Btu/lb°F])
δ_{ij} = Kronecker's delta tensor [-]
ε = dissipation of turbulent kinetic energy [m²/s³] ([ft²/s³])
$\varepsilon(s)$ = emissivity of inside surface of wall [-]
θ = temperature of air [°C] ([°F])
θ_o = outdoor temperature [°C] ([°F])
θ_p = temperature at a node adjacent to wall [°C] ([°F])
θ_r = average room air temperature [°C] ([°F])
θ_w = inside surface temperature of i th cell [°C] ([°F])
κ = von Kármán's constant [-]
ν = molecular viscosity [m²/s] ([ft²/s])
ν_t = turbulent eddy viscosity [m²/s] ([ft²/s])
ρ = density of air [kg/m³] ([lb/ft³])

Subscripts & Model constants

w = wall surface p = a node adjacent to wall.

$\sigma_k = 1.0$, $\sigma_\varepsilon = 1.3$, $\sigma_\theta = 1.0$
$C_{\varepsilon 1} = 1.59$, $C_{\varepsilon 2} = 2.0$, $C_D = 0.09$

Table 1. Thermal conductance used for calculation of heat flux.

Wall-1, Wall-3 (excluding windows)	0.599 W/m² K (0.106 Btu/ft²h°F)
Wall-2, Wall-4	0.283 W/m²K (0.050 Btu/ft²h°F)
Ceiling	0.338 W/m²K (0.058 Btu/ft²h°F)
Window-1, Window-2, Window-3	6.232 W/m²K (1.098 Btu/ft²h°F)
Natural ventilation rate	0.5

Outside film coefficient was set at 23.256 W/m²K (4.098 Btu/ft²h°F) for ceiling, 9.302 W/m²K (1.639 Btu/ft²h°F) for floor and 15.000 W/m²K (2.643 Btu/ft²h°F) for others.

Table 2. Heat supply and heat loss obtained from experiment.

	Case 1	Case 2	Case 3
Area to be heated (in Fig. 2)	A, B, C, D	B, C	A, B
Outside temperature (to) [°C] ([°F])	2.6 (36.7)	2.6 (36.7)	2.6 (36.7)
Average room temperature (ta) [°C] ([°F])	20.2 (68.4)	19.7 (67.5)	17.8 (64.0)
Temperature difference (tdif=ta-to) [°C] ([°F])	17.6 (63.7)	17.1 (62.8)	15.2 (59.4)
Mean radiant temperature (MRT) [°C] ([°F])	19.2 (66.6)	18.8 (65.8)	16.7 (62.1)
Operative temperature (OT) [°C] ([°F])	19.7 (67.5)	19.3 (66.7)	17.3 (63.1)
Average heated floor surface temp [°C] ([°F])	25.3 (77.5)	26.5 (79.7)	26.5 (79.7)
Supplied water temperature [°C] ([°F])	57.0 (134.6)	69.3 (156.7)	71.7 (161.1)
Returned water temperature [°C] ([°F])	48.3 (118.9)	61.4 (142.5)	64.6 (148.3)
Heat supply from hot water [W] ([Btu/h])	1119 (3818)	1096 (3740)	1043 (3559)
Ratio of heating effect [W/K] ([Btu/h°F])	63.6 (120.5)	64.1 (121.4)	68.6 (129.9)

Table 3. Heat exchange on inside surface. (Unit [W (Btu/h)])

(a) Case 1

	Convection-Cal.	Radiation-Cal.	Sum-Cal.	Sum-Exp.
Wall-1	253.6 (865.3)	297.3 (1014.4)	550.9 (1879.8)	414.7 (1415.0)
Wall part	90.2 (307.8)	119.3 (407.1)	209.5 (714.8)	87.8 (299.6)
Windows part	163.4 (557.5)	178.0 (607.4)	341.5 (1165.3)	326.9 (1115.4)
Wall-2	53.0 (180.8)	49.9 (170.3)	102.9 (351.1)	70.6 (240.9)
Wall-3	158.6 (541.2)	165.2 (563.7)	323.8 (1104.9)	285.1 (972.8)
Wall part	59.7 (203.7)	60.6 (206.8)	120.3 (410.5)	53.5 (182.6)
Windows part	98.9 (337.5)	104.6 (356.9)	203.5 (694.4)	231.6 (790.3)
Wall-4	23.1 (78.8)	16.3 (55.6)	39.4 (134.4)	46.8 (159.7)
Ceiling	54.9 (187.3)	118.9 (405.7)	173.8 (593.0)	128.1 (437.1)
Natural ventilation	-	-	-	174.0 (593.7)
Total of heat loss	543.2 (1853.5)	647.6 (2209.7)	1190.8 (4063.2)	1119.3 (3819.2)
Floor (supply)	-565.2 (-1928.5)	-619.5 (-2113.8)	-1184.7 (-4042.4)	-1119.3 (-3819.2)
Heat balance	-22.0 (-75.1)	28.1 (95.9)	6.1 (20.8)	

(b) Case3

	Convection-Cal.	Radiation-Cal.	Sum-Cal.	Sum-Exp.
Wall-1	216.4 (738.4)	244.3 (833.6)	460.7 (1572.0)	353.0 (1204.5)
Wall part	76.3 (260.3)	97.5 (332.7)	173.8 (593.0)	76.1 (259.7)
Windows part	140.1 (478.0)	146.8 (500.9)	286.9 (978.9)	276.9 (944.8)
Wall-2	41.3 (140.9)	28.4 (96.9)	69.7 (237.8)	61.7 (210.5)
Wall-3	109.9 (375.0)	149.7 (510.8)	259.5 (885.5)	263.9 (900.5)
Wall part	33.5 (114.3)	52.3 (178.5)	85.8 (292.8)	50.3 (171.6)
Windows part	76.4 (260.7)	97.3 (332.0)	173.7 (592.7)	213.6 (728.8)
Wall-4	47.8 (163.1)	-8.4 (-28.7)	39.4 (134.4)	37.9 (129.3)
Ceiling	45.5 (155.3)	67.1 (229.0)	112.6 (384.2)	111.4 (380.1)
Floor unheated	43.8 (149.5)	74.9 (255.5)	118.7 (405.0)	64.4 (220.4)
Natural ventilation	-	-	-	150.3 (512.8)
Total of heat loss	504.6 (1721.8)	555.9 (1896.8)	1060.5 (3618.6)	1042.7 (3557.9)
Floor (supply)	-515.4 (-1758.6)	-535.0 (-1825.5)	-1050.3 (-3618.6)	-1042.7 (-3557.9)
Heat balance	-10.8 (-36.9)	18.0 (61.4)	10.2 (34.8)	

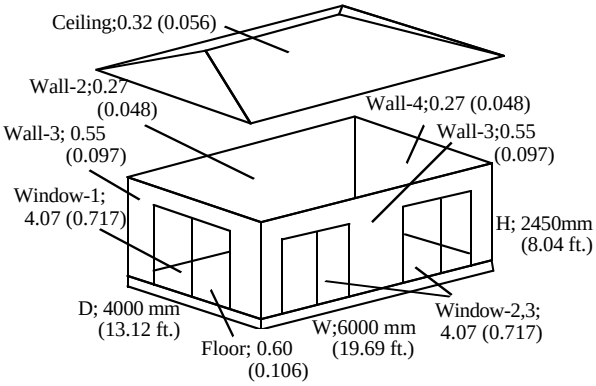

Figure 1 Full-scaled room and the U-values (Unit : W/ m²K [Btu/ft²h°F])

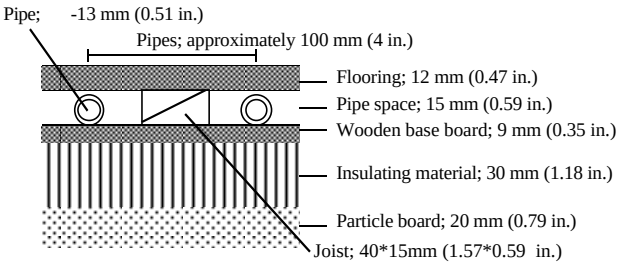

Figure 3 Structure and materials of floor heater.

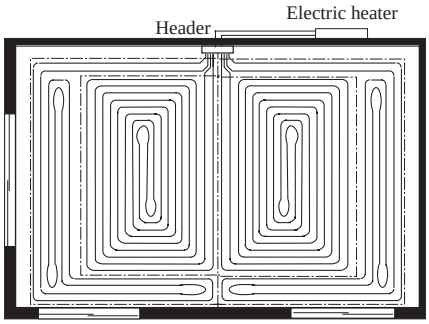

(a) Embedding of pipe.

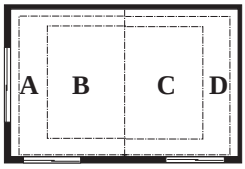

(b) Division of heated area.

Figure 2 Piping for hot water circulation.

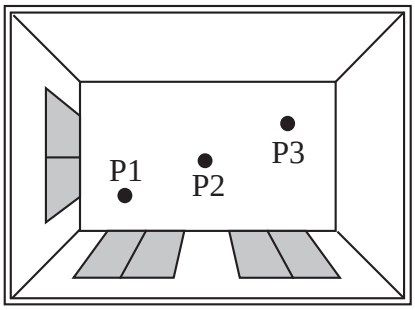

Measured position illustrated in Figures.

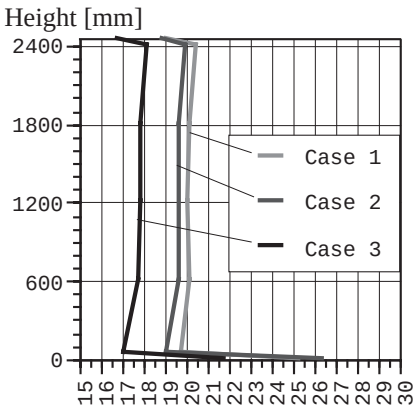

(a) Average values (Measurement).

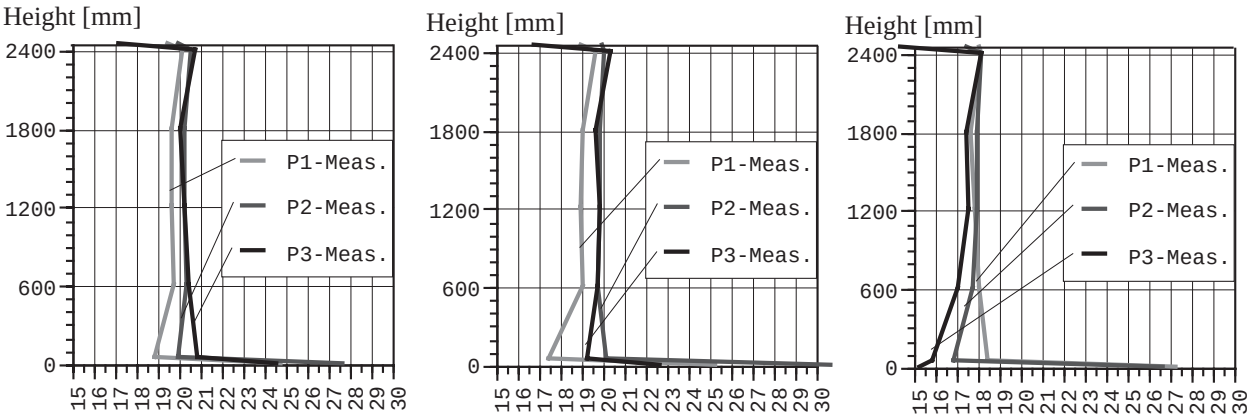

(b-1) Case 1. **(b-2)** Case 2. **(b-3)** Case 3.

(b) Measured values at P1, P2, P3.

Figure 4 Vertical temperature profiles obtained by measurement.

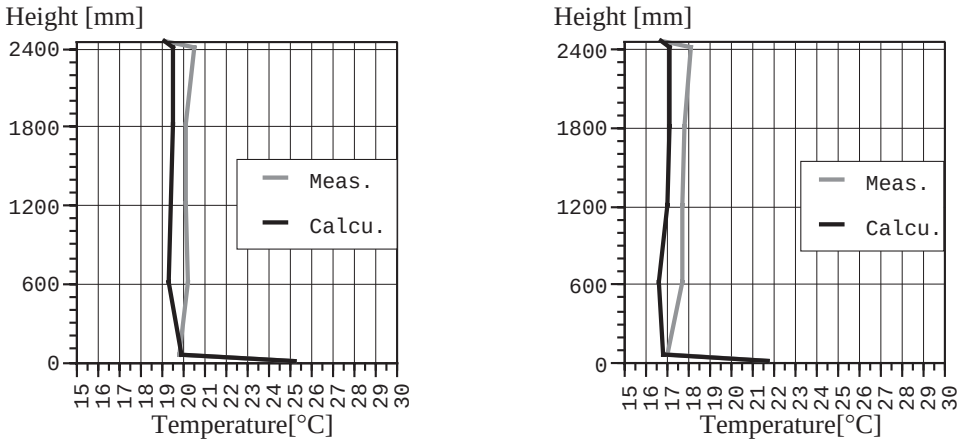

(a-1) Case 1. **(a-2)** Case 3.

(a) Comparison of average profiles.

Figure 5 Comparison of vertical temperature profiles between measurements and calculations.

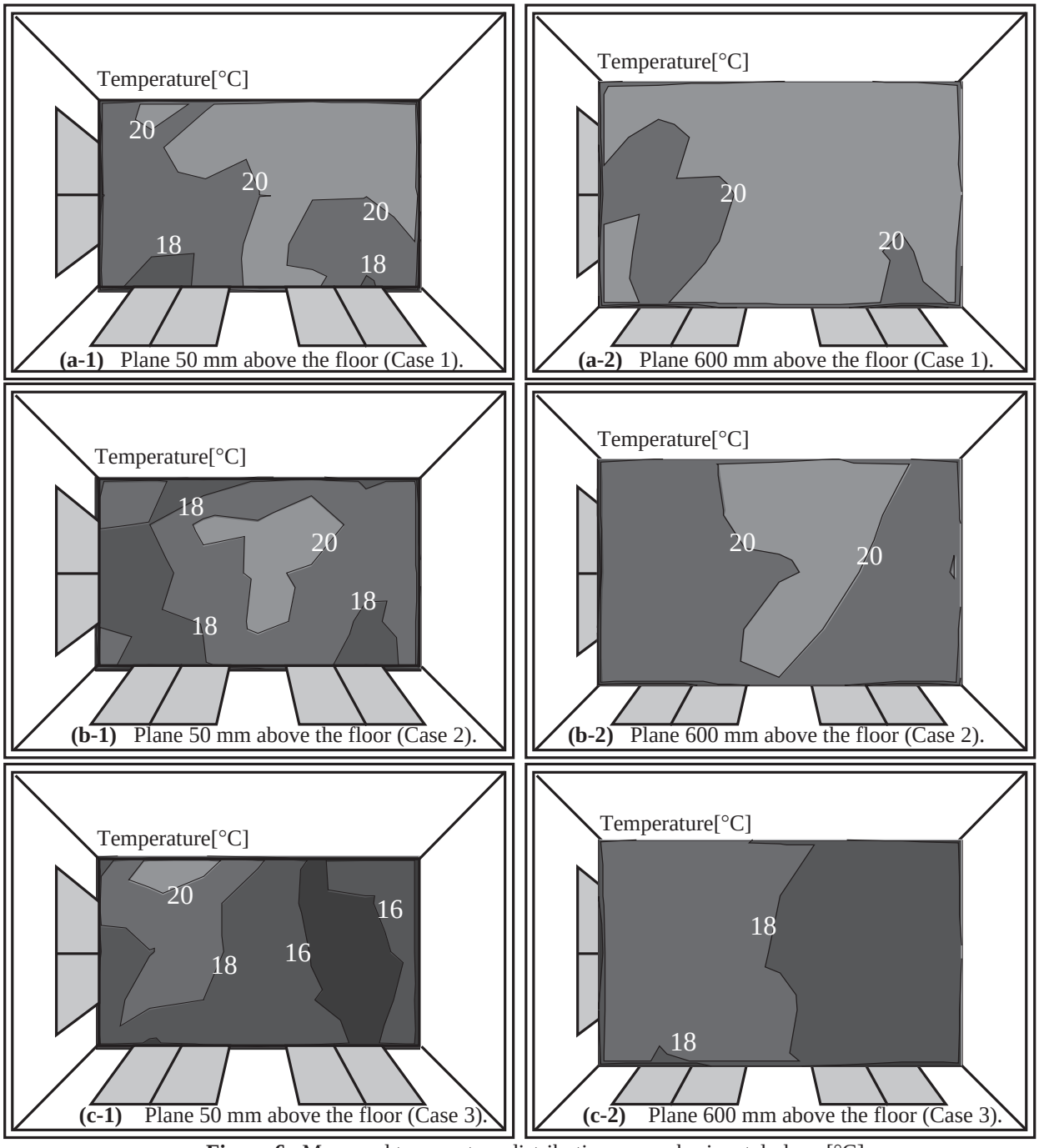

Figure 6 Measured temperature distribution across horizontal plane [°C].

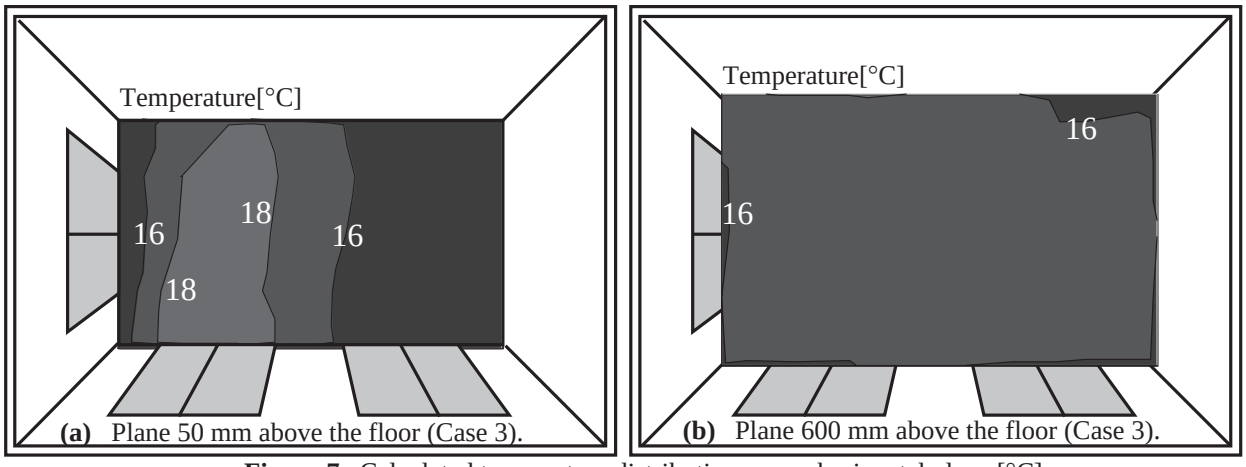

Figure 7 Calculated temperature distribution across horizontal plane [°C].